

Observation of quasi bound states in open quantum wells of cesiated p-doped GaN surfaces

Mylène Sauty^{1,2}, Jean-Philippe Banon^{1,3}, Nicolas M. S. Lopes¹,
Tanay Tak⁴, James S. Speck⁴, Claude Weisbuch^{1,4}, Jacques Peretti¹
¹*Laboratoire de Physique de la Matière Condensée, CNRS,
Ecole polytechnique, Institut Polytechnique de Paris, 91120 Palaiseau, France*
²*Service de Physique de l'Etat condensé (SPEC),
Université Paris-Saclay, CEA-CNRS, F-91191, Gif-sur-Yvette, France*
³*Laboratoire Charles Fabry, Institut d'Optique Graduate School,
CNRS, Université Paris-Saclay, 91127 Palaiseau, France*
⁴*Materials Department, University of California, Santa Barbara, California 93106, USA*

(Dated: March 31, 2025)

The quantized electron states in the downward band bending region (BBR) at the surface of cesiated p-type GaN are investigated. We theoretically predict the existence of metastable resonant states in the BBR with an intrinsic life-time around 20 fs. Their experimental observation requires access to the empty conduction band of the cesiated semiconductor, which is possible with near-bandgap photoemission spectroscopy. The energy distribution of the photoemitted electrons shows contributions coming from electrons accumulated into the resonant states at energies which agree with calculations.

The quantized energy states in narrow, triangular-shaped space-charged layers formed at metal-insulator-semiconductor (MIS) interfaces and their influence on carriers mobilities and transport properties have been investigated for more than 50 years [1–3]. Under specific band alignments, similar triangular quantum wells form at semiconductor-semiconductor interfaces, as in modulation doped (MD) AlGaAs/GaAs or AlGaIn/GaN interfaces, leading to high mobility materials, novel phenomena such as the Quantum Hall Effect (although first observed in Si MOS structures) and electronic devices such as high electron mobility transistors (HEMTs) [4, 5]. Such narrow triangular wells for carriers can also form at the free surface of semiconductors depending on doping and surface states. Typically, the clean surface of p-doped GaAs or GaN displays a downwards band bending region (BBR) due to the mid gap pinning of the Fermi level at the surface [6].

The energy position and properties of these quantized states have been particularly studied in MIS inversion layers or MD structures, when the well contains carriers, forming a 2D electron or hole gas (2DEG or 2DHG) [2–5]. In this situation of a closed triangular well filled with carriers, several approaches for investigating quantized states have been developed. Optical techniques were used to measure photoluminescence from the 2DEG formed at the AlGaAs/GaAs and AlGaIn/GaN interfaces [7–9], as well as the 2DHG at the GaN/AlGaIn interface [10]. Electrical measurements, in particular magneto-transport measurements of Shubnikov–de Haas oscillations, gave access to the energy separation between the quantized states and to the carrier concentrations in each energy level, in AlGaIn/GaN [11], or at the free surface of Te [12]. Finally, photoemission spectroscopy allowed the direct measurement of the energy position,

momentum dispersion and carrier dynamics in the quantized states of surface inversion layers, typically in InAs, InSb or InSe where the pinning of the Fermi level could be tuned with surface impurities, dopants or alkali metals [13–16].

The energy landscape for carriers around the surface BBR of a semiconductor can, however, be significantly different from the case of inversion layers, as for example at the free surface of a p-doped semiconductor after the deposition of a monolayer of an alkali metal, a widely used technique for photocathodes [6, 17, 18]. In this case, the semiconductor workfunction is reduced such that the vacuum level is below the bulk conduction band minimum, to the situation of negative electron affinity (NEA), while the Fermi level is pinned at mid-gap, well below the conduction band minimum. In this configuration, the triangular well formed by the surface BBR is non-confining on the vacuum side, hereafter referred to as the open quantum well. In this work, we show that although this potential map induces a continuum of states in the BBR, there still exists resonant states manifested by local maxima in the density of states. The experimental observation of these resonant states requires to probe the empty conduction band of the semiconductor, contrarily to the investigation of inversion layers described previously. There has been some attempts to observe such states using low energy photoemission spectroscopy on GaAs photocathodes [19–21]. However, their contributions to the observed photoemission current could not be distinguished from those originating from the bulk states of the semiconductor [22], because of the narrow bandgap of GaAs and the use of an above bandgap excitation energy, as will be discussed later. In this work, we investigate instead the resonant states in the BBR of cesiated p-GaN, a semiconductor with a much larger

bandgap than GaAs. The p-doping of GaN induces a downwards BBR of an amplitude of more than 1.5 eV over a few nm only, leading to quantization energies of the order of the eV, much larger than in GaAs. We observe the signature of the resonant states in the energy distribution of the photoemitted electrons. In particular, below bandgap excitation allows to clearly distinguish them from the bulk contribution.

Theoretically, the question of the existence and properties of quantized states in the surface BBR of cesiated GaAs photocathodes was addressed early on using analytical effective mass calculations [20, 23]. However, a vanishing envelope wave-function was considered at the interface, as for infinite quantum wells, not really accounting for the non-confining nature of the BBR well on the vacuum side. More recently, numerical works on photoemission have used the effective mass model with a jump of effective mass at the interface, in order to find a transmission coefficient to be implemented in Spicer's three-step model [24, 25], but we are not aware of a subsequent study of the metastable quantized states induced by this open quantum well.

Here, we investigate numerically the local density of states (LDOS) in the open well at the free surface of cesiated p-doped GaN. Resonances can be predicted by determining the local maxima of the density of states [26]. The calculation is achieved within an open system framework in which the electronic states in the semiconductor are represented in the envelope function approximation and are coupled to the plane wave states in the vacuum (see Sec. I in the Supplemental Material (SM) for more details). The potential experienced by the conduction band electrons, V_c , corresponds to the conduction band minimum (CBM) in the semiconductor and to the vacuum level position (here 1.5 eV above the Fermi level E_F) in vacuum. The Cs layer is modeled by a triangular potential barrier of height 5 eV, corresponding to the GaN workfunction before cesiation, and a thickness of 0.3 nm [18, 27] [28]. The spatial variation of the potential in the semiconductor close to the surface was computed by solving the Poisson equation assuming a Mg doping with concentration of $1 \times 10^{20} \text{ cm}^{-3}$, consistent with the experimental sample studied below, while imposing the Fermi level to be pinned at mid gap at the surface (Sec. I.C in the SM). As shown by the white solid line in Fig. 1(a), this potential does not strictly form a well for electrons which can tunnel through the thin potential barrier at the surface. For such open systems, it is convenient to work with the Green's function G associated to the effective mass Schrödinger equation, defined by (SM Sec. I.B)

$$\frac{\hbar^2}{2} \nabla \cdot \left[\frac{\nabla G}{m(z)} \right] (\mathbf{r}, \mathbf{r}', E) + (E - V_c(z)) G(\mathbf{r}, \mathbf{r}', E) = \delta(\mathbf{r} - \mathbf{r}'), \quad (1)$$

and subjected to outgoing wave radiation conditions at

infinity. Here E denotes the energy variable, and \mathbf{r} and \mathbf{r}' may be viewed as an observation and a source point, respectively. The system being invariant by translations in the (x, y) -plane, the Green's function may be expressed as $G(\mathbf{r}_{\parallel} - \mathbf{r}'_{\parallel}, z, z', E)$ where $\mathbf{r}_{\parallel} = (x, y)$ denotes the projection of a point \mathbf{r} in the (x, y) -plane. The two-dimensional Fourier transform of the Green's function in the (x, y) -plane, $\bar{G}(\mathbf{p}, z, z', E)$, then satisfies the equation

$$\frac{\hbar^2}{2} \frac{d}{dz} \left[\frac{1}{m(z)} \frac{d\bar{G}}{dz} \right] (\mathbf{p}, z, z', E) + \left[E - V_c(z) - \frac{\hbar^2 p^2}{2m(z)} \right] \bar{G}(\mathbf{p}, z, z', E) = \delta(z - z'). \quad (2)$$

The LDOS is obtained from the imaginary part of the Green's function as [29]

$$\text{LDOS}(\mathbf{r}, E) = -\frac{1}{\pi} \text{Im} G(\mathbf{r}, \mathbf{r}, E), \quad (3)$$

or in the (x, y) -Fourier space as

$$\text{LDOS}(\mathbf{p}, z, E) = -\frac{1}{\pi} \text{Im} \bar{G}(\mathbf{p}, z, z, E). \quad (4)$$

The latter expression measures the number of states with in-plane wave vector \mathbf{p} and contributing at point z , per unit length and unit energy. Computing the LDOS thus requires solving Eq. (2) for the Green's function for a given energy E and a given wave vector \mathbf{p} (see Sec. II of the SM for the numerical method).

The calculated LDOS as a function of space and energy at vanishing in-plane wave vector ($p = 0$) is shown in Fig. 1(a). We observe that, at energies higher than the bulk CBM, the electronic wave functions are propagating plane waves in the vacuum and in the bulk of the semiconductor, as attested by the periodic spatial oscillations in the LDOS [30]. For energies lower than the bulk CBM, electronic wave functions are also propagating plane waves in the vacuum and are evanescent waves in the bulk of the semiconductor. In the BBR, although there exists a continuum of states, the LDOS exhibits local maxima at specific energies, which we identify as resonant states. Their energies of about 2.4 eV and 3.0 eV above the Fermi level can be extracted from the LDOS integrated spatially over the semiconductor in Fig. 1(b). These states are metastable states in the BBR. They may be thought in a semi-classical picture as states for which electrons undergo many reflections within the BBR before being transmitted into the vacuum [31]. This is analogous to photons in a leaky Fabry-Perot cavity in optics, or more generally the so-called quasi-normal modes in any structured open photonic system [32, 33]. By fitting Lorentzian line shapes to the density of states, the life-time of the two resonant states are estimated to be about 18 fs and 23 fs, for the lowest and highest energy resonant state, respectively.

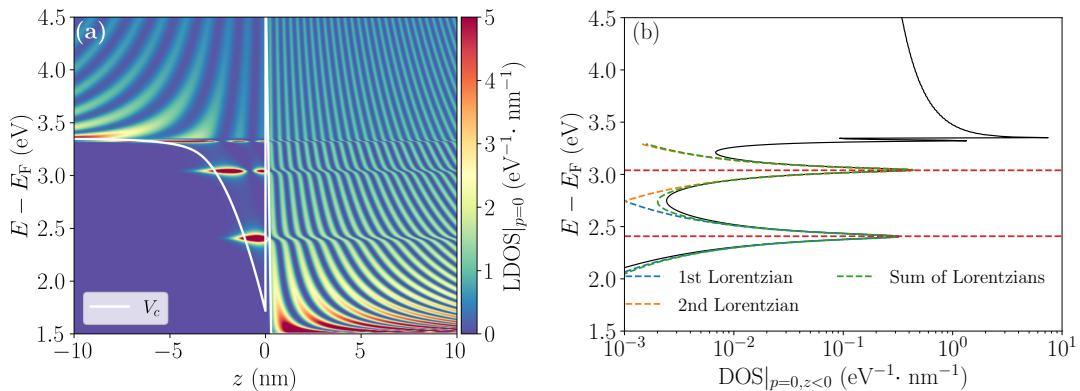


FIG. 1. (a) 1D LDOS at vanishing transverse wave-vector ($p = 0$) calculated with the envelope function approximation. The potential seen by electrons is marked by the white line, and corresponds to the CBM in the semiconductor and to the vacuum level E_{vac} in the vacuum. The LDOS shows that electron wavefunctions have a plane wave structure both in vacuum for all energies and in the semiconductor for energies higher than the bulk CBM. For energies lower than the bulk CBM in the BBR region, there is still a continuum of states but two resonant states appear at 2.4 eV and 3.0 eV. (b) 1D DOS at $p = 0$, obtained by integration of the LDOS over $z < 0$. The DOS is fitted with the sum of two Lorentzian functions of the form $A_1/[(E - E_1)^2 + (\Gamma_1/2)^2] + A_2/[(E - E_2)^2 + (\Gamma_2/2)^2]$. The fitted energy and spectral width of the resonances are $E_1 = 2.4$ eV, $E_2 = 3.0$ eV, $\Gamma_1 = 37.7$ meV and $\Gamma_2 = 28.2$ meV. The corresponding life-times are $\tau_1 = \hbar/\Gamma_1 = 17.5$ fs and $\tau_2 = 23.4$ fs.

Note that, our numerical calculations in the open system framework remove restrictions from the early calculations [20, 23]. They show in particular that the envelope wave-function does not strictly vanish at the interface at resonances as can be seen in Fig. 1(a), in contrast to the assumption usually encountered in the literature [20, 23]. In general, it is expected that the resonance condition should depend both on the details of the potential on both sides of the interface and on the effective mass jump, as will be described in a future article. Perhaps more importantly, early calculations [19, 20, 23] did not address the spectral broadening or life-time of the resonant states which is fundamentally related to their metastability due to their leakage into vacuum. The Green's function approach in an open system presented here gives this information.

Experimentally, the existence of resonant states in the BBR of cesiated p-GaN was investigated using low energy photoemission, as schematically shown in Figure 2. The exposition of the sample to near-bandgap photons excites electrons in the semiconductor conduction band, that can be emitted into the vacuum after transport and relaxation processes, in the bulk and in the BBR [6, 34]. Emission to the vacuum is permitted by the low vacuum level due to the Cs monolayer at the sample surface [27].

For direct bandgap semiconductors, with near but above bandgap excitation, photoelectrons are generated in the first tens to first hundreds of nm of the material. Along their transport to the surface, they relax to the minima of the conduction band, which act as accumulation points and appear as characteristic features in the energy distribution of photoemitted electrons [22, 35–38], signature of the semiconductor DOS.

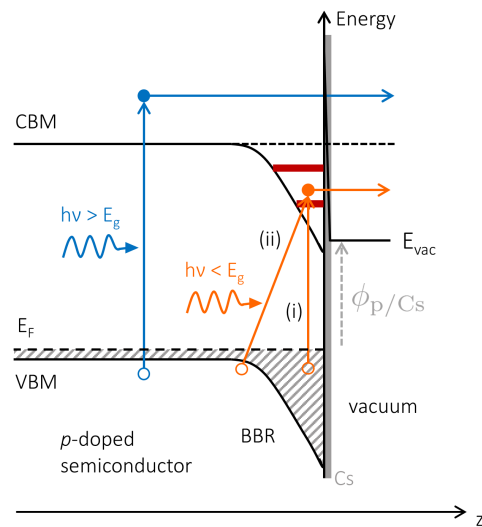


FIG. 2. Schematic of the photoemission processes for a p-type semiconductor in negative electron affinity, for near-bandgap excitation. The blue arrows schematize above bandgap excitation, while the orange ones picture below bandgap excitation and absorption in the BBR.

On the contrary, with below bandgap light excitation, band-to-band absorption in the bulk does not occur. A photoemission current can then arise only from absorption from defect states (process (i) in Figure 2) [39], or from Franz-Keldysh absorption assisted by the strong electric field in the BBR (process (ii) in Figure 2). After their excitation close to the surface, electrons do not experience any transport step. They are confined in the quasi-well formed by the BBR and can only relax in avail-

able states, before being emitted into vacuum.

The studied sample is a MOCVD-grown *c*-plane heterostructure. It consists in 200-nm p-GaN (Mg: $5 \times 10^{19} \text{ cm}^{-3}$) with surface overdoping (Mg: $\approx 1 \times 10^{20} \text{ cm}^{-3}$ on the last 10 nm close to the surface), grown on n-GaN (Si: $6 \times 10^{18} \text{ cm}^{-3}$) and UID GaN on a sapphire substrate. The sample first underwent a chemical cleaning in piranha (H_2SO_4 and H_2O_2 mixture, 3:1 ratio) and HCl-isopropanol solutions [40]. After being inserted in the ultra high vacuum (UHV) chamber (base pressure 5×10^{-11} mbar), it was annealed for about 10 minutes at 350°C . To achieve NEA, cesium was deposited on its surface, while monitoring the photoemission current for an excitation energy corresponding to the semiconductor bandgap (3.4 eV). A complete Cs monolayer was obtained [27].

The energy distribution of the photoemitted electrons was then recorded using a UV-enhanced lamp associated to bandpass filters, with a bandwidth of 10 nm, for an excitation power of about 200 μW . The electrons were collected by an energy analyzer specifically designed for low energy electrons [41], with an energy resolution of 50 meV. Derivatives of the energy distribution curves were obtained numerically, and the resolution was decreased to 80 meV due to a smoothing step in the data processing.

The energy distribution curves (EDC) obtained for excitation energies between 2.85 eV and 4.13 eV are shown in Figure 3, along with their numerical derivatives (DEDC). Since GaN bandgap is 3.4 eV, half of the curves correspond to below bandgap excitation. For clarity, both EDC and DEDC have been translated along the Y axis, the EDC translation being proportional to the incident photon energy. For all curves, the vacuum level, which corresponds to the low energy threshold of the EDC, is at about 1.5 eV above the Fermi level, confirming that surface NEA is achieved. The high energy threshold of the EDC corresponds to the energy $E_F + h\nu$ (marked in dashed line on the EDC plot).

Depending on excitation energy, different contributions appear. For all excitation energies, the lowest energy contribution, marked S in the EDC, corresponds to the continuum of electrons excited close to the surface [37] (process shown by orange arrows in Figure 2). In addition, for above bandgap excitation ($h\nu > 3.4$ eV), the contribution from electrons accumulated in the bulk conduction band minimum (CBM), noted Γ , appears as a positive bump in the EDC, whose high energy side forms a negative feature in the DEDC, shaded in blue. This Γ contribution has a high energy threshold at the bulk CBM position, and extends to lower energy due to the electron energy losses when crossing the BBR [37]. In between these two contributions (S and Γ), two other peaks appear progressively when the excitation energy is increased. They are shaded in grey in the DEDC, and labelled (1) and (2). They are particularly enhanced for an

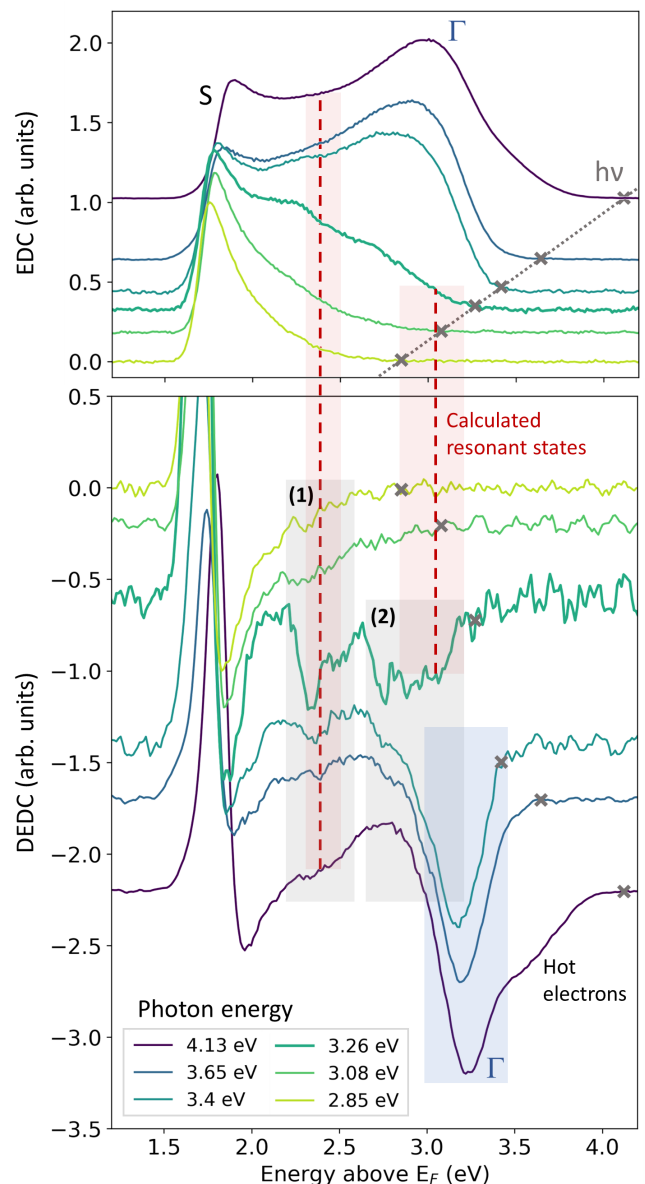


FIG. 3. Energy distribution curves (EDC) and numerical derivative (DEDC) on GaN for near bandgap excitation, from 2.85 to 4.13 eV. The vacuum level is at about 1.5 eV above the Fermi level (E_F), meaning that NEA is achieved. For photon energies $h\nu > 3.4$ eV, the Γ contribution from electrons accumulated in the bulk conduction band minimum (CBM), appears at identical position in all curves (blue shaded area). Additional contributions at lower energy than Γ are marked by the two grey-shaded area in the DEDC.

excitation energy of 3.26 eV, for which they are both accessible energetically by electrons, but are not yet hidden by the Γ contribution. We attribute these two contributions to the resonant states in the open well formed by the BBR and the sample surface.

The energy position of the resonant states in the BBR obtained by our LDOS calculation for a surface overdop-

ing of $1 \times 10^{20} \text{ cm}^{-3}$ are reported as dashed red lines on the experimental curves in Figure 3, at 2.4 eV and 3.0 eV above the Fermi level. The red shaded area around the calculated resonant states corresponds to energy positions obtained for doping levels between $5 \times 10^{19} \text{ cm}^{-3}$ and $2 \times 10^{20} \text{ cm}^{-3}$, reflecting the uncertainty on the exact surface doping level. Overall, the calculated energy positions match the 2 contributions observed in the DEDCs. Note that, the shape of the contribution of a resonant state in the DEDC results from an interplay between the escape of the electrons accumulated in the state and their relaxation towards the continuum. In GaN, the optical phonon scattering rate is of the order of 10-30 fs [42–44]. This is comparable to the lifetimes of the calculated resonant states of 18 and 23 fs, and can explain the broadening of the states contributions in the experimental curves.

Finally, these BBR resonant states are clearly distinguishable only for specific excitation energies below the material bandgap, for which they can be populated but their contribution is not hidden by the numerous, energy-relaxed, bulk electrons. In the previous attempts to observe such states in GaAs photocathodes [19–21], such condition was harder to obtain due to the smaller bandgap of GaAs, and we believe that in the published experimental data, the resonant states contribution could not be distinguished from the bulk Γ contribution, as we explain in more details in Sec. III of the SM.

In this work, we have investigated, both experimentally and theoretically, the density of states in the surface BBR of cesiated p-type GaN. We have shown that despite the opening of the potential well by the reduction of the workfunction by the Cs layer, resonant metastable states exist in the energy continuum extending from the vacuum level to the CBM in the bulk. On the experimental side, the combination of a below bandgap excitation and a large bandgap material permits the observation of such states without them being hidden by the large contribution of bulk electrons. On the theory side, our Green’s function approach allows the calculation of the states lifetimes.

We thank Lucia Reining and Marcel Filoche for fruitful discussions. This work was supported by the French National Research Agency (ANR, TECCLON Grant No. ANR-20-CE05-0037-01) and by the Simons Foundation (Grants No. 1027114 C.W., No. 601944 and 601937 J.-P. B.). Support at UCSB was provided by the Solid State Lighting and Energy Electronics Center (SSLEEC); U.S. Department of Energy under the Office of Energy Efficiency & Renewable Energy (EERE) Award No. DE-EE0009691; the National Science Foundation (NSF) RAISE program (Grant No. DMS-1839077); the Simons Foundation (Grant No. 601952).

- [1] J. R. Schrieffer, Mobility in inversion layers: Theory and experiment, in *Semiconductor Surface Physics* (University of Pennsylvania Press, 1957) pp. 55–69.
- [2] T. Ando, A. B. Fowler, and F. Stern, Electronic properties of two-dimensional systems, *Rev. Mod. Phys.* **54**, 437 (1982).
- [3] F. Stern, Quantum properties of surface space-charge layers, *C R C Crit. Rev. Solid State Sci.* **4**, 499 (1973).
- [4] R. Dingle, H. L. Störmer, A. C. Gossard, and W. Wiegmann, Electron mobilities in modulation-doped semiconductor heterojunction superlattices, *Appl. Phys. Lett.* **33**, 665 (1978).
- [5] E. A. Jones, F. F. Wang, and D. Costinett, Review of Commercial GaN Power Devices and GaN-Based Converter Design Challenges, *IEEE Journal of Emerging and Selected Topics in Power Electronics* **4**, 707 (2016).
- [6] J. Scheer and J. van Laar, GaAs-Cs: A new type of photoemitter, *Solid State Commun.* **3**, 189 (1965).
- [7] J. P. Bergman, Q. X. Zhao, P. O. Holtz, B. Monemar, M. Sundaram, J. L. Merz, and A. C. Gossard, Time-resolved measurements of the radiative recombination in GaAs/Al_xGa_{1-x}As heterostructures, *Phys. Rev. B* **43**, 4771 (1991).
- [8] J. P. Bergman, T. Lundström, B. Monemar, H. Amano, and I. Akasaki, Photoluminescence related to the two-dimensional electron gas at a GaN/AlGaN heterointerface, *Appl. Phys. Lett.* **69**, 3456 (1996).
- [9] R. Kaneriyay, C. Karmakar, M. K. Sahu, P. Basu, and R. Upadhyay, Low temperature photoluminescence study for identification of intersubband energy levels inside triangular quantum well of AlGaIn/GaN heterostructure, *Microelectron. J.* **131**, 105660 (2023).
- [10] L. Méchin, F. m. c. Médard, J. Leymarie, S. Bouchoule, J.-Y. Duboz, B. Alloing, J. Zuñiga Pérez, and P. Disseix, Experimental demonstration of a two-dimensional hole gas in a GaN/AlGaIn/GaN based heterostructure by optical spectroscopy, *Phys. Rev. B* **109**, 125401 (2024).
- [11] Z. W. Zheng, B. Shen, R. Zhang, Y. S. Gui, C. P. Jiang, Z. X. Ma, G. Z. Zheng, S. L. Guo, Y. Shi, P. Han, Y. D. Zheng, T. Someya, and Y. Arakawa, Occupation of the double subbands by the two-dimensional electron gas in the triangular quantum well at Al_xGa_{1-x}N/GaN heterostructures, *Phys. Rev. B* **62**, R7739 (2000).
- [12] Bouat, J. and Thuillier, J.C., Calculation of surface quantum levels in tellurium inversion layers, *J. Phys. France* **39**, 1193 (1978).
- [13] L. O. Olsson, C. B. M. Andersson, M. C. Håkansson, J. Kanski, L. Ilver, and U. O. Karlsson, Charge Accumulation at InAs Surfaces, *Phys. Rev. Lett.* **76**, 3626 (1996).
- [14] V. Y. Aristov, G. Le Lay, V. M. Zhilin, G. Indlekofer, C. Grupp, A. Taleb-Ibrahimi, and P. Soukiassian, Direct measurement of quantum-state dispersion in an accumulation layer at a semiconductor surface, *Phys. Rev. B* **60**, 7752 (1999).
- [15] D. Wutke, M. Garb, A. Krawczyk, A. Mielczarek, N. Olszowska, M. Rosmus, and J. J. Kolodziej, Band structure of a nonparabolic two-dimensional electron gas system, *Phys. Rev. B* **107**, 155139 (2023).
- [16] Z. Chen, J. Sjakste, J. Dong, A. Taleb-Ibrahimi, J.-P. Rueff, A. Shukla, J. Peretti, E. Papalazarou, M. Marsi, and L. Perfetti, Ultrafast dynamics of hot carriers in a

- quasi-two-dimensional electron gas on InSe, PNAS **117**, 21962 (2020).
- [17] W. E. Spicer, Negative affinity 3–5 photocathodes: Their physics and technology, Appl. Phys. **12**, 115 (1977).
- [18] X. Wang, M. Wang, Y. Liao, L. Yang, Q. Ban, X. Zhang, Z. Wang, and S. Zhang, Negative electron affinity of the GaN photocathode: a review on the basic theory, structure design, fabrication, and performance characterization., J. Mat. Chem. C **9**, 13013 (2021).
- [19] D. Orlov, V. Andreev, and A. Terekhov, Elastic and inelastic tunneling of photoelectrons from the dimensional quantization band at a p+-GaAs-(Cs,O) interface into vacuum, JETP Lett. **71**, 151 (2000).
- [20] V. Korotkikh, A. Musatov, and V. Shadrin, Influence of size-effect quantization of energy levels in semiconductors on the photoelectron emission, JETP Lett. **11**, 652 (1978).
- [21] X. Jin, Analysis of electron emission from GaAs(Cs,O) by low energy electron microscopy, Jpn. J. Appl. Phys. **54**, 101201 (2015).
- [22] H.-J. Drouhin, C. Hermann, and G. Lampel, Photoemission from activated gallium arsenide. I. Very-high-resolution energy distribution curves, Phys. Rev. B **31**, 3859 (1985).
- [23] L. G. Gerchikov and A. V. Subashiev, Resonance enhancement of the photoemission from semiconductors with negative electron affinity, J. Appl. Phys. **80**, 6008 (1996).
- [24] A. G. Zhuravlev, A. S. Romanov, and V. L. Alperovich, Photon-enhanced thermionic emission from p-GaAs with nonequilibrium Cs overlayers, Appl. Phys. Lett. **105**, 251602 (2014).
- [25] V. Alperovich, D. Kazantsev, A. Zhuravlev, and L. Shvartsman, Photoemission and photon-enhanced thermionic emission: Effect of jump in electron mass, Appl. Surf. Sci. **561**, 149987 (2021).
- [26] N. Moiseyev, *Non-Hermitian Quantum Mechanics* (Cambridge University Press, 2011).
- [27] M. Sauty, C. W. Johnson, T. Tak, W. Y. Ho, Y. C. Chow, J. S. Speck, A. K. Schmid, C. Weisbuch, and J. Peretti, Investigation of the cesium activation of GaN photocathodes by low-energy electron microscopy, Phys. Rev. Appl. **22**, 034005 (2024).
- [28] Note that, a change in the values of the barrier height and thickness within a range of an eV and a few Å, respectively, does not affect significantly the simulation results.
- [29] E. Akkermans and G. Montambaux, *Mesoscopic Physics of Electrons and Photons* (Cambridge University Press, 2007).
- [30] Note that we represent here the envelope function and not the full Bloch wave function in the semiconductor.
- [31] N. Hatano, K. Sasada, H. Nakamura, and T. Petrosky, Some Properties of the Resonant State in Quantum Mechanics and Its Computation, Prog. Theor. Phys. **119**, 187 (2008).
- [32] P. Lalanne, W. Yan, K. Vynck, C. Sauvan, and J.-P. Hugonin, Light Interaction with Photonic and Plasmonic Resonances, Laser & Photonics Rev. **12**, 1700113 (2018).
- [33] S. Both and T. Weiss, Resonant states and their role in nanophotonics, Semiconductor Science and Technology **37**, 013002 (2021).
- [34] W. E. Spicer, Photoemissive, Photoconductive, and Optical Absorption Studies of Alkali-Antimony Compounds, Phys. Rev. **112**, 114 (1958).
- [35] Y. Lassailly, P. Chiaradia, C. Hermann, and G. Lampel, Experimental photoemission results on the low-energy conduction bands of silicon, Phys. Rev. B **41**, 1266 (1990).
- [36] J. Peretti, H.-J. Drouhin, D. Paget, and A. Mircéa, Band structure of indium phosphide from near-band-gap photoemission, Phys. Rev. B **44**, 7999 (1991).
- [37] M. Piccardo, L. Martinelli, J. Iveland, N. Young, S. P. DenBaars, S. Nakamura, J. S. Speck, C. Weisbuch, and J. Peretti, Determination of the first satellite valley energy in the conduction band of wurtzite GaN by near-band-gap photoemission spectroscopy, Phys. Rev. B **89**, 235124 (2014).
- [38] M. Sauty, N. M. S. Lopes, J.-P. Banon, Y. Lassailly, L. Martinelli, A. Alhassan, Y. C. Chow, S. Nakamura, J. S. Speck, C. Weisbuch, and J. Peretti, Localization Effect in Photoelectron Transport Induced by Alloy Disorder in Nitride Semiconductor Compounds, Phys. Rev. Lett. **129**, 216602 (2022).
- [39] A. A. Pakhnevich, V. V. Bakin, A. V. Yaz'kov, G. Shaibler, S. Shevelev, O. E. Tereshchenko, A. S. Yaroshevich, and A. S. Terekhov, Energy distributions of photoelectrons emitted from p-GaN (Cs, O) with effective negative electron affinity, JETP Lett. **79**, 479 (2004).
- [40] O. Tereshchenko, G. Shaibler, A. Yaroshevich, S. Shevelev, A. Terekhov, V. Lundin, E. Zavarin, and A. Besyul'kin, Low-temperature method of cleaning p-GaN (0001) surfaces for photoemitters with effective negative electron affinity, Phys. Solid State **46**, 1949 (2004).
- [41] H. Drouhin and M. Eminyan, Simple concepts in the measurement of the energy distribution and spin polarization of an electron beam, Rev. Sci. Instrum. **57**, 1052 (1986).
- [42] S. Marcinkevičius, T. K. Uždavinyš, H. M. Foronda, D. A. Cohen, C. Weisbuch, and J. S. Speck, Intervalley energy of GaN conduction band measured by femtosecond pump-probe spectroscopy, Phys. Rev. B **94**, 235205 (2016).
- [43] K. T. Tsen, D. K. Ferry, A. Botchkarev, B. Sverdlov, A. Salvador, and H. Morkoç, Direct measurements of electron-longitudinal optical phonon scattering rates in wurtzite GaN, Appl. Phys. Lett. **71**, 1852 (1997).
- [44] F. Bertazzi, M. Moresco, and E. Bellotti, Theory of high field carrier transport and impact ionization in wurtzite GaN. Part I: A full band Monte Carlo model, J. Appl. Phys. **106**, 063718 (2009).